Carbohydrate Polymers 89 (2012) 935–941

Contents lists available at SciVerse ScienceDirect

Carbohydrate Polymers

journal homepage: www.elsevier.com/locate/carbpol

In vitro characterisation of chitosan based xerogels for potential buccal delivery of proteins

Isaac Ayensu, John C. Mitchell, Joshua S. Boateng*

Department of Pharmaceutical, Chemical and Environmental Sciences, School of Science, University of Greenwich at Medway, Chatham Maritime, Kent ME4 4TB, UK

ARTICLE INFO

Article history:
Received 11 December 2011
Received in revised form 9 April 2012
Accepted 12 April 2012
Available online 21 April 2012

Keywords:
Thiolated-chitosan
Lyophilisation
Mucoadhesion
Buccal delivery
Protein

ABSTRACT

Chitosan and thiolated-chitosan based xerogels have been prepared by lyophilising aqueous gels of the polymers incorporating glycerol, D-mannitol and BSA with an annealing process. Analytical characterisation was by circular dichroism, infrared spectroscopy, X-ray diffraction and scanning electron microscopy. Swelling capacities of 1110 ± 23.3% and 480 ± 18.2% were obtained for the chitosan and TG-chitosan xerogels respectively. Thiolation caused improved in vitro mucoadhesive properties by demonstrating peak adhesive force of 4.5 ± 0.7 and 5.8 ± 0.2 N, and total work of adhesion of 6.5 ± 1.0 and 19 ± 0.8 mJ for chitosan and thiolated-chitosan xerogels respectively. In vitro drug dissolution studies using Bradford's assay showed BSA release of 91.5 ± 3.7% and 94.4 ± 7.3% from the chitosan and thiolated-chitosan xerogels respectively. These results demonstrate the potential of developing lyophilised thiolated-chitosan xerogels with optimised mucoadhesion characteristics for buccal mucosa delivery of protein based drugs.

1. Introduction

The concept of mucoadhesion has gained increased attention in pharmaceutical technology over the past two decades and might provide opportunities for novel, highly efficient dosage forms, suitable for buccal drug delivery (Thanou, Nihot, Jansen, Verhoef, & Junginger, 2001).

Chitosan (Fig. 1(a)) a polyaminosaccharide derived from chitin was discovered 200 years ago (Muzzarelli et al., 2012). Chitosan exhibits mucoadhesive properties and is often used to enhance the residence time of a drug in the mucosal membrane thereby increasing drug bioavailability. Its hydrophilicity and the presence of functional amino groups and a net cationic charge make chitosan a suitable polymer for the intelligent delivery of macromolecular compounds, such as proteins and genes. The poor solubility of chitosan in neural or alkaline medium however limits its usage. The solubility in aqueous solvents of up to a pH of 6.5 is however attainable via the protonation of the glucosamine unit to produce soluble $R\text{-}NH_3^+$ (Kumar, Muzzarelli, Muzzarelli, Sashiwa, & Domb, 2004).

The unique properties exhibited by chitosan have further been improved by derivatization of the amine functionality. Recently, it has been shown that polymers with thiol groups (thiomers) possess much higher adhesive properties than polymers generally considered mucoadhesive (Bernkop-Schnürch, 2000). Sulfhydryl bearing agents can be covalently attached to this primary amino group via the formation of amide bonds where the carboxylic acid group of the ligand, such as thioglycolic acid (TGA) is conjugated with chitosan via the primary amino group, mediated by a water soluble carbodiimide (Fig. 1) (Kast & Bernkop-Schnürch, 2001). The improved mucoadhesive properties of TG-chitosan are explained by the formation of stronger covalent bonds between thiol groups of the polymer and cysteine rich sub-domains of glycoproteins present in the mucus layer (Leitner, Walker, & Bernkop-Schnürch, 2003; Snyder, Reddy, Cennerazzo, & Field, 1983).

A number of variable parameters capable of altering the interaction between chitosan and the mucosal layer can affect the mucoadhesive property of the polymer. These include but are not limited to polymer molecular weight (Andrew, Laverty, & Jones, 2009; Tiwari, Goldman, Sause, & Madan, 1999), polymer concentration (Solomonidou, Cremer, Krumme, & Kreuter, 2001) and method of drying. Grabovac, Guggi, and Bernkop-Schnürch (2005) reported that the method of drying is vital as it influenced the mucoadhesive potential of polymers. They showed that lyophilised TG-chitosan produced greater mucoadhesion than others dried by precipitation in organic solvents.

The addition of plasticizers to polymeric dosage forms also imparts flexibility, reduces brittleness, increases toughness and improves flow. It achieves this by interposing itself between the

Abbreviations: ATR-FTIR, attenuated total reflectance Fourier transform infrared; BSA, bovine serum albumin; CD, circular dichroism; DTT, dithiotreitol; GPC, gel permeation chromatography; PAF, peak adhesive force; PBS, phosphate buffered saline; SEM, scanning electron microscopy; TA, texture analyser; TGA, thermo-gravimetric analysis; TWA, total work of adhesion; XRD, X-ray diffractometry.

* Corresponding author. Tel.: +44 0208 331 8980; fax: +44 0208 331 9805.
E-mail addresses: j.s.boateng@gre.ac.uk, joshboat@hotmail.com (J.S. Boateng).

0144-8617/$ – see front matter © 2012 Elsevier Ltd. All rights reserved.
http://dx.doi.org/10.1016/j.carbpol.2012.04.039

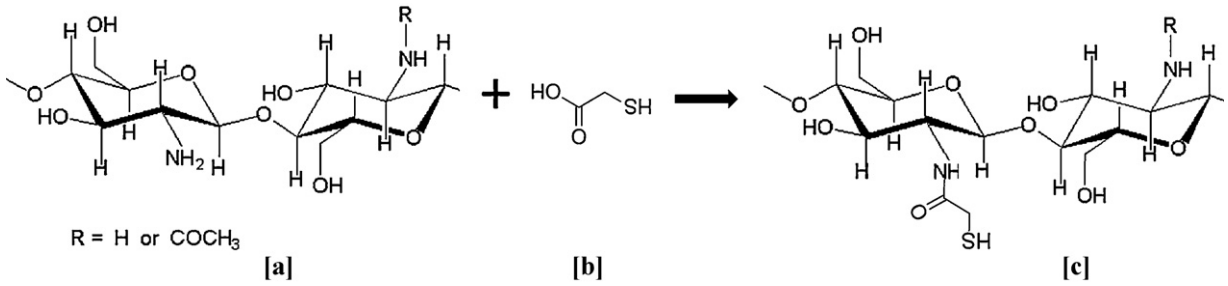

Fig. 1. Synthesis of TG-chitosan: (a) chitosan, (b) TGA, and (c) TG-chitosan.

polymer chains and interacting with polymer functional groups to reduce interaction and intermolecular cohesive forces between the polymer chains (Boateng et al., 2009).

The aim of this study was to formulate and evaluate the characteristics of lyophilised chitosan and TG-chitosan xerogels as potential drug delivery systems via the buccal mucosa.

2. Experimental

2.1. Materials

Chitosan (medium molecular weight, 190–310 kDa, 75–85% deacetylated), BSA (mol wt ~ 66 kDa), glycerol, D-mannitol, Coomassie blue (Bradford reagent), thioglycolic acid, N-(3-dimethylaminopropyl)-N-ethyl carbodiimide hydrochloride (EDAC), L-cysteine hydrochloride, 5,5′-dithiobis(2-nitrobenzoic acid) (Ellman's reagent), dithiotreitol (DTT), pullulan 200,000 standard, Spectra/Por® Float-A-Lyzer® G2 dialysis device (8–10 kDa molecular weight cut-off; cellulose ester membrane) and mucin from bovine submaxillary gland, Type I-S were all obtained from Sigma (Gillingham, UK). Pulverised gelatine was purchased from Fischer Scientific (Loughborough, UK). All other reagents were of analytical grade and were used without further purification.

2.2. TG-chitosan synthesis

TG-chitosan was synthesised as previously described (Saboktakin, Tabatabaie, Maharramov, & Ramazanov, 2011). 500 mg of chitosan was dissolved in 50 ml of 0.1 M HCl. An equivalent of 500 mg of thioglycolic acid (TGA) was added, the pH adjusted to 5 with 1 M NaOH and 50 mM EDAC added in order to activate the carboxylic moieties of TGA. After an incubation period of 4 h at room temperature with continuous stirring, the resulting thiolated polymer was dialysed to remove unconjugated TGA against different aqueous media. The order of removal was as follows: 8 h against 5 l of 5 mmol/l HCl, 8 h against 5 mmol/l HCl containing 1% NaCl (twice) to prevent ionic interactions between the cationic chitosan and the anionic sulfhydryl ligand and finally 8 h against 5 l of 5 mmol/l HCl (twice in the dark). This was done using a Spectra/Port® Float-A-Lyzer® G2 dialysis device (Sigma, Gillingham, UK). The dialysed products were either used directly for gel formulation or lyophilised (Table 1) and stored at 4 °C pending further analysis. The amount of thiol group immobilized was determined by Ellman's reaction and standard cysteine HCl curve ($r^2 > 0.99$) as previously reported (Bernkop-Schnürch, Guggi, & Pinter, 2004). The average molecular weights (Mw) of chitosan and TG-chitosan were monitored with Agilent technologies 1100 series gel permeation chromatography (GPC) analysis system equipped with an isocratic pump and a refractive index detector. Samples were dissolved in buffer 0.2 M CH_3COOH/0.1 M CH_3COONa and eluted through Tosoh TSK-GEL PW column (7.8 mm × 300 mm, 10 μm) at a flow rate of 1 ml/min at 30 °C using the same buffer as mobile phase and pullulan 200,000 as standard. The resulting GPC data were analysed with Agilent Chemstation software.

2.3. Gel formulation and freeze drying

Formulations were prepared by adding 10% (relative to dry polymer weight) each of glycerol and mannitol as plasticizer and cryoprotectant respectively to the recovered dialysed gel and loaded with 50% BSA as a model protein drug. The final gel containing 1% (w/v) TG-chitosan was stirred continuously for 30 min at room temperature to obtain a homogeneous mixture which was kept at room temperature to remove all air bubbles. Unmodified chitosan gel was used as the control.

6.5 g each of the chitosan and TG-chitosan gels prepared above were transferred into moulds (diameter 35 mm) (Thermo Fisher Scientific, Leicester, UK) and freeze dried using an automated lyophilisation cycle incorporating an annealing process (Table 1) on a Virtis AdVantage XL 70 freeze dryer (Biopharma Process Systems, Winchester, UK). The end of the primary drying (ice sublimation) stage was determined by probes signalling equal product and shelf temperatures. The cycle was based on previous preliminary thermal characterisation by DSC (Ayensu, Mitchell, & Boateng, 2012). The resulting lyophilised xerogels were stored over silica gel in desiccators to maintain the desired low water content ideal for maintaining protein stability, till ready for characterisation. Xerogels obtained directly from freeze-drying dialysed TG-chitosan gel were evaluated against those formulated from lyophilised TG-chitosan powder.

2.4. Analytical characterisation of chitosan and TG-chitosan xerogels

ATR-FTIR spectra of chitosan and TG-chitosan were acquired on an Excalibur series FTS 3500 ARX Fourier transform infrared spectrophotometer (FTIR), equipped with Specac Golden gate (Varian, Oxford, UK). The spectra were collected at a resolution of 1.5 cm^{-1} with 16 scans per spectrum using a wave number range of 600–4000 cm^{-1}.

The conformational structure of BSA was examined by far-UV CD. Spectra of a 1 mg/ml solution of native BSA in 0.1 M PBS (pH 6.8) as the negative control or BSA released from the xerogels were recorded at 25 °C from wavelength range $240 \geq \lambda \geq 190$ with bandwidth 1 nm, time-per-point 0.5 s, and cell path-length of 0.1 mm using CD spectroscopy (Chirascan, Applied Photophysics). The mean residue ellipticity $[\theta]_{mrw,k}$ was determined using Eq. (1) below:

$$[\theta]_{mrw,k} = \frac{MRW \times \theta_k}{10 \times d \times c} \quad (1)$$

where MRW is the mean residue weight, θ_k is the observed ellipticity (°) at wavelength k, d is the pathlength (cm), and c is the concentration (g/ml) (Kelly, Jess, & Price, 2005).

Table 1
Lyophilisation cycle with an annealing step.

Step	Thermal treatment (annealing)			Primary drying process		
	Temperature (°C)	Time (min)	Ramp/hold, R/H	Temperature (°C)	Time (min)	Vacuum (mTorr)
1	+5	30	H	−25	420	50
2	−5	30	H	−25	420	20
3	−40	120	H	Secondary drying process		
4	−20	180	H	+20	360	10
5	−40	180	H			

A D8 Advantage X-ray diffractometer (Bruker AXS GmbH, Karlsure, Germany) was employed to study the crystallinity (or otherwise) of the xerogels. The transmission diffractograms were acquired with Diffrac plus XRD Commander over a start to end diffraction 2θ angle of 5–45°, scan speed of 0.4 s and step size of 0.02. The operating conditions were 40 kV and 40 mA with Cu Kα radiation. Data was processed with EVA software for native BSA powder, unmodified chitosan powder, drug loaded chitosan and TG-chitosan xerogels.

Morphology of xerogels was studied with a Cambridge Stereoscan S-360 SEM (Class one equipment, London, UK) after sputter coating for 120 s at 1 kV and 30 mA with gold (Edwards Sputter Coater S150B). Images were acquired at an accelerating voltage of 20 kV, a working distance of 15 mm and processed with i-scan2000 software.

2.5. Drug loading efficiency

The drug loading efficiency of the xerogels was estimated from the ratio of actual and initial BSA loading. 35 mg of drug loaded xerogel was dissolved in 25 ml of 1% (v/v) acetic acid. The solution was magnetically stirred for 10 min at room temperature at 50 rpm to avoid bubble formation. 50 μl of the solution was withdrawn and treated with 1 ml Bradford's reagent and the absorbance measured at 595 nm and 450 nm for linearization of absorbance (Ernst & Zor, 2010) using a Multiskan EX microplate photometer equipped with Ascent software (Thermo Scientific, Hampshire, UK). The amount of BSA was determined by interpolation from the linearized calibration curve ($r^2 > 0.99$). Each experiment was run in triplicate.

2.6. Swelling capacity

The swelling capacities of the lyophilised chitosan-BSA and TG-chitosan-BSA xerogels were determined by incubating the samples in 25 ml of 0.1 M PBS solution (pH 6.8 ± 0.1) at 37 ± 0.1 °C with or without reducing agent, 10 mM dithiotreitol (DTT). The xerogels were weighed initially and the swelling characteristics observed over predetermined time intervals. The samples were taken out, blotted off carefully between tissue papers to remove the surface liquid droplets and reweighed to a constant weight. The swelling capacity was calculated as follows:

$$\text{Swelling capacity } (\%) = 100 \times \frac{S_s - S}{S} \quad (2)$$

where S_s is the weight of the hydrated xerogel, and S is the initial weight of xerogel.

2.7. Moisture content

The percentage residual moisture content of the lyophilised xerogels was estimated by thermogravimetric analysis using Thermal Advantage TGA 2950 (TA Instruments, Crawley, UK). A constant rate of heating at 15 °C/min from ambient temperature to a maximum of 150 °C was applied with a constant stream of dry nitrogen to xerogels weighing between 3 and 6 mg in a previously tared 70 μl aluminium crucible. TA Universal Analysis 2000 programme was used to determine the percentage weight loss from a second derivative plot.

2.8. In vitro mucoadhesion

Mucoadhesive measurements were performed on the lyophilised chitosan-BSA and TG-chitosan-BSA xerogels with a TA.HD.*Plus* Texture Analyser (Stable Micro Systems, Surrey, UK) fitted with a 5 kg load cell in tension mode. The samples ($n = 4$) were attached to a 75 mm diameter probe with double sided adhesive tape. A model buccal mucosal substrate made of 6.67% (w/v) gelatine solution allowed to set as solid gel in a petri-dish (diameter 88 mm) and equilibrated with 2% mucin solution (adjusted to pH of 6.8 ± 0.1) was used for the in vitro measurement. The mucosal substrate was placed on the instrument platform and the probe, lined with xerogel, was set to approach the model mucosal surface with the following settings: pre-test speed 0.5 mm/s; test speed 0.5 mm/s; post-test speed 1.0 mm/s; applied force 1 N; contact time 60.0 s; trigger type auto; trigger force 0.05 N and return distance of 10.0 mm. The peak adhesive force (PAF) required to detach the xerogel from the mucosal substrate, the total work of adhesion (TWA), represented by the area under the curve (AUC) and the cohesiveness (distance of travel) of the samples were determined by utilising Texture Exponent 32 software. The influence of thiolation on adhesive strength was also investigated.

2.9. In vitro drug dissolution studies

The drug loaded xerogels were immersed in beakers containing 50 ml of PBS (pH of 6.8 ± 0.1) solution as dissolution medium at 37 ± 1 °C, covered and stirred at 150 rpm with a magnetic stirrer. 50 μl of the medium was withdrawn at set time intervals and replaced with the same amount of PBS to maintain a constant volume. The sampled medium was treated with 1 ml Bradford's reagent and the absorbance measured as described previously in Section 2.7. The concentration of the BSA released from the xerogels was estimated from the linearized calibration curve ($r^2 > 0.99$).

2.10. Statistical data analysis

A two tailed Student's *t*-test at 95% confidence interval (*p*-value < 0.05) as the minimal level of significance was used to evaluate the data statistically.

3. Results and discussion

3.1. TG-chitosan synthesis and characterisation

TGA was bound to chitosan via amidation between the carboxylic group of TGA and primary amino groups of the polymer (Fig. 1). The reactivity of the primary amino group at the 2-position of glucosamine subunit of chitosan was exploited for the immobilization of thiol groups. The process was performed

at a pH ≤ 5 to prevent the formation of disulphide bonds by air oxidation as the reactive thiolate anion concentration for the oxidation of thiol groups is low at this pH. Nuclear magnetic resonance (NMR) was not suitable for evaluating the level of free thiol groups and disulphide bonds since two equivalent carbons and two equivalent protons of thioglycolic acid appeared overlapped with those of chitosan in a NMR spectrum as reported by (Juntapram, Praphairaksit, Siraleartmukul, & Muangsin, 2012; Lee et al., 2007). As in their study, spectrophotometric assay using Ellman's reagent was employed in the determination of the amount of reduced and oxidized thiol groups immobilized (Hornof, Kast, & Bernkop-Schnürch, 2003) without previous quantitative reduction of disulfide bonds with borohydride. The TG-chitosan conjugate had 236 ± 26 μmol thiol groups per gram of polymer. According to Sreenivas and Pai (2009), a degree of modification of 25–250 mmol thiol groups per gram of chitosan results in the highest improvement in the mucoadhesive and permeation enhancing properties of these TG-chitosans. GPC analysis for monitoring the polymer Mw before and after derivatization showed differences in the calculated Mw. The difference in the calculated Mw of chitosan (196,744 Da) and TG-chitosan (200,708 Da) after the conjugation reaction could be attributed to the addition of thioglycolic acid molecules unto the chitosan chains. This suggests that polymeric chains may not have been degraded during the synthesis process.

3.2. Gel formulation and freeze drying

Flexible, tough, non-brittle and porous lyophilised chitosan-BSA and TG-chitosan-BSA xerogels have been produced. The 10% D-mannitol as a cryoprotectant prevents crystallisation of BSA, maintaining the protein as part of a high viscosity and slightly flexible freeze-concentrated liquid phase. During the freezing stages, hydrogen bonds form between the protein molecules and the cryoprotectant as water molecules are displaced. Therefore the protein maintains its native physiological structure (and function), independent of an aqueous environment. The presence of glycerol leads to enhanced flexibility as freeze induced stress generated during lyophilisation is lowered, allowing the xerogels to accommodate the stress. A combination of two different cryoprotectants (or plasticizers), each at reduced concentration, has a better outcome since undesirable effects such as brittleness (D-mannitol) or stickiness (glycerol) produced by higher concentrations of a single agent is reduced (Ayensu et al., 2012). Faster water vapour transport, shorter primary drying time and elegant porous xerogels were achieved by incorporating an annealing process during the freezing stage. Annealing also promotes ice crystals growth and complete crystallisation of mannitol from the amorphous phase so that metastable mannitol does not crystallise on storage, which will affect product stability.

The dialysed gel produced elegant xerogels and prevented double lyophilisation, saving time and cost. Since no significant differences were observed between the characteristics of the xerogels from the two processes, industrial applicability of direct formulation would be of more benefit than manufacture via lyophilised TG-chitosan powder.

3.3. Analytical characterisation of chitosan and TG-chitosan xerogels

The ATR-FTIR spectra (Fig. 2) show the respective absorption peaks of chitosan and TG-chitosan at 1666.35 and 1618.27 cm^{-1} which corresponds to the characteristic amide I band (Qin et al., 2006). The peaks at 1556.55 cm^{-1} and 1522.67 cm^{-1} were assigned to amide II band (CN stretching and NH bend) present in both chitosan and TG-chitosan. The absorption bands at 3271.26 cm^{-1} and 3255.48 cm^{-1} are for NH stretch and the weak peak at 2525.68 cm^{-1}

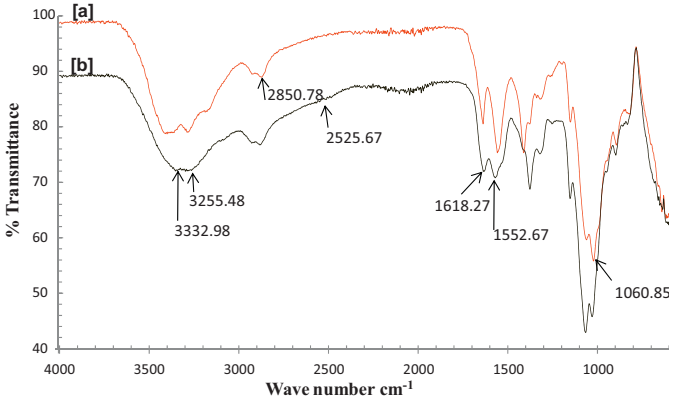

Fig. 2. ATR-FTIR spectra of (a) chitosan and (b) TG-chitosan.

corresponds to SH (Saboktakin et al., 2011), confirming the conjugation between SH and primary amine of chitosan in TG-chitosan. The absorption bands at 3342.63 cm^{-1} and 3332.98 cm^{-1} were for chitosan-OH and TG-chitosan-OH respectively, the band at 997.19–1060.85 cm^{-1} was due to CO and the 2850–2900 cm^{-1} band resulted from aliphatic CH stretch. CD was employed to investigate the conformational structure of native BSA and that present in the xerogel. The CD profile of native BSA and BSA released from the xerogels, both in PBS at pH 6.8 in far UV range are shown in Fig. 3. The native BSA had two minima around 209 and 222 nm; the first band was assigned to the α-helical structure, while the second band was assigned to the β-structure. These results are consistent with the structure of BSA reported by Quiming, Vergel, Nicolas, and Villanueva (2005). The ratios between the mean residue ellipticity at 209 and 222 nm ($[\theta]_{209}/[\theta]_{222}$) were 1.10, 1.10 and 1.10 for (i) native BSA, BSA released from the annealed, (ii) chitosan-BSA and (iii) TG-chitosan-BSA respectively. The similarity of the far-UV CD spectra and the mean residue ellipticity obtained confirmed the conformational stability of BSA in the lyophilised xerogels. Fig. 4 shows XRD transmission diffractograms of plain chitosan powder, native BSA, chitosan-BSA and TG-chitosan-BSA xerogels. XRD analysis was used to study the physical form (crystalline or amorphous) since these properties are reported to affect water uptake and biodegradability characteristics of polymers (Prabaharan & Gong, 2008). Crystalline chitosan showed its characteristic intense peak at 2θ of 20° (Nagahama et al., 2009). The formulated xerogels however, had the intensity of this peak minimized, leaving the peak at 2θ between 22° and 24° which was a shoulder to the right of the main chitosan peak (Fig. 4a). These results revealed the existence of amorphous structures that resulted from chemical modification of chitosan following formulation with amorphous BSA (Fig. 4d),

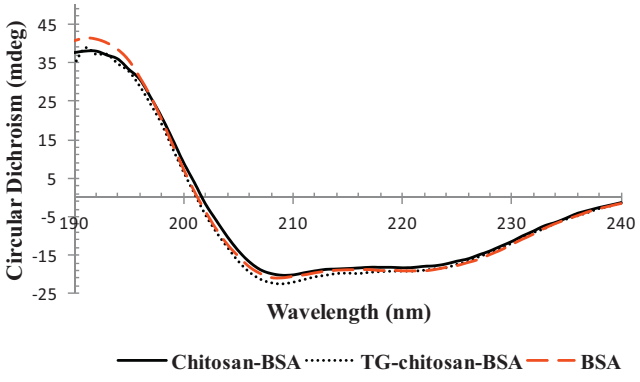

Fig. 3. CD spectra of native BSA, chitosan-BSA and TG-chitosan-BSA xerogels.

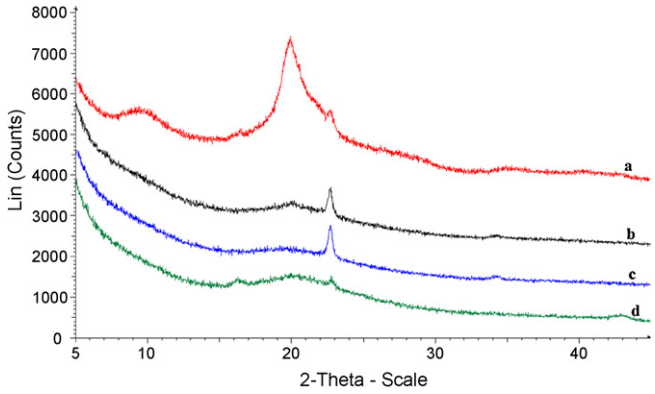

Fig. 4. XRD-transmission diffractogram of (a) plain chitosan powder, (b) TG-chitosan-BSA xerogel, (c) chitosan-BSA xerogel and (d) native BSA powder.

and other excipients, leading to the alteration of the original crystalline chitosan. They also show that the freeze-drying procedure did not alter the amorphous structures formed during gel formulation prior to the freezing step during which ice crystal formation occurs. The final amorphous xerogel could help in maintaining the stability of the model protein drug which was originally added as an amorphous powder and also enhance the mucoadhesive properties of the formulated polymer (Prabaharan & Gong, 2008) as a result of improved hydration and reduced rigidity (Kasper & Freiss, 2011). Fig. 5 shows representative micrographs of the lyophilised xerogels. The micrographs from the SEM show the effect of annealing on the pore size. The sublimation of larger ice crystals formed from the merging of smaller ice crystals due to annealing, results in xerogels with large pores. The chitosan-BSA xerogels formed a fibrous, sponge-like, porous interconnecting polymer network with circular pores that were regularly distributed. The TG-chitosan-BSA xerogels also formed a fibrous, sponge-like, porous interconnecting polymer network but with smaller pore sizes and a more irregular pore distribution. The presence of low molecular weight compounds such as glycerol, D-mannitol and thioglycolic acid with high affinity for water is likely to have an effect on ice crystal ripening during the slow freezing process, which affects ice crystal size and subsequently pore size, hence the difference observed in the morphologies of the chitosan-BSA and TG-chitosan-BSA xerogels. Such differences in morphology such as pore size can affect functional properties such as rate of hydration, swelling, mucoadhesion and subsequent drug release rates. This arises primarily from the differences in rate of water ingress, swelling and subsequent diffusion of drug from swollen matrix (Boateng et al., 2010).

3.4. Drug loading efficiency

Table 2 shows the drug loading efficiencies for the unmodified chitosan-BSA and TG-chitosan-BSA xerogels. Thiolation did not have a significant effect on the drug loading efficiency as both xerogels had similar values. In addition, chitosan and TG-chitosan did not interfere with the reagent used for the BSA quantification. The difference in the drug loading efficiencies of the xerogels was not statistically significant ($p > 0.05$). The fibrous and porous networks of the lyophilised cakes allowed for the higher drug loading efficiency compared with other mucosal formulations such as solvent cast films (Boateng et al., 2010).

3.5. Swelling capacity

The difference in the swelling capacities of the chitosan-BSA xerogel ($1110 \pm 23.3\%$) and TG-chitosan-BSA xerogel ($480 \pm 18.2\%$) (Table 2) was statistically significant ($p < 0.0001$) in the absence of a disulphide reducing agent (DTT). The swelling capacity of the chitosan-BSA xerogel reached the maximum value within 30 min of incubation, which was due to the increased hydrophilicity of chitosan in the presence of glycerol and mannitol. In addition, the enhanced pore size allowed for a higher rate of water ingress with a swelling capacity more than twofold that of the TG-chitosan. It was observed that the rate of water ingress and swelling was slower for the TG-chitosan-BSA xerogel which prevented the formation of an excessively hydrated structure. This could be attributed to oxidation of free thiol groups to inter- and intra-molecular disulphide bonds in PBS at a higher pH of 6.8 which subsequently limited the hydration process. However in the presence of a disulphide reducing agent (DTT), a dramatic increase in swelling capacity was observed for the TG-chitosan xerogel (Table 2) giving evidence that the swelling characteristic is driven by the formation of internal disulphide linkages in the TG-chitosan xerogels. Mucoadhesive xerogels are expected to be hydrated on the underlying mucosal tissue by water absorption, swelling and capillary action resulting in stronger adhesion.

3.6. Moisture content

The residual moisture content of the chitosan-BSA and TG-chitosan-BSA xerogels are shown in Table 2. The weight loss

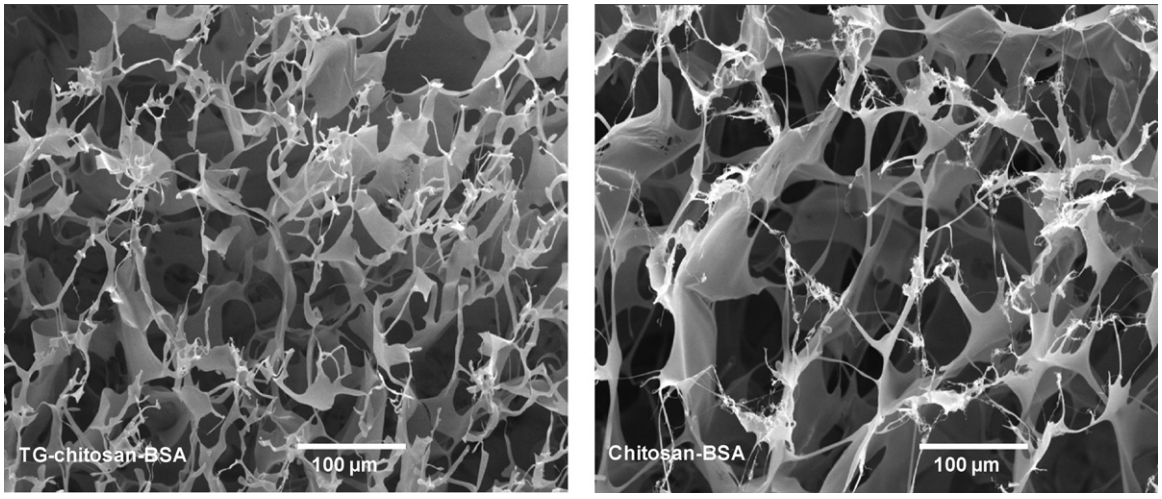

Fig. 5. Representative SEM micrographs showing chitosan-BSA and TG-chitosan-BSA xerogels (magnification: 200×).

Table 2
Results of drug loading, swelling capacity, moisture content and texture analysis of xerogels containing BSA ($n = 4$, mean ± S.D.).

Samples	Drug loading (%)	Swelling capacity (%)		Moisture content (%)	Texture analysis (in vitro mucoadhesion)		
		Without DTT	With DTT		PAF (N)	TWA (mJ)	Cohesiveness (mm)
Chitosan-BSA	91.6 ± 4.0	1110 ± 23.3	1057 ± 20.2	1.8 ± 0.7	4.5 ± 0.7	6.5 ± 1.0	4.4 ± 0.6
TG-chitosan-BSA	94 ± 1.6	480 ± 18.2	1087 ± 5.1	1.8 ± 0.1	5.8 ± 0.2	19 ± 0.8	4.8 ± 1.0

determined for the xerogels occurred during the constant rate of heating between 60 °C and 120 °C due to loss of bound water. Attaining adequate residual moisture content for the xerogels was vital as lower water content reduces molecular mobility and increases shelf life by avoiding premature hydration of the active protein drug.

3.7. In vitro mucoadhesion

The in vitro mucoadhesive performance (Table 2) was measured by evaluating the PAF, the TWA and the cohesiveness of the xerogels. The chitosan-BSA xerogels had lower PAF compared to the TG-chitosan-BSA xerogels with a difference that was statistically significant ($p < 0.02$). This difference was expected to be much higher, however, the combined effect of the absorbent properties of glycerol, D-mannitol and the enhanced intermolecular hydrogen bonding with the gelatine substrate employed could have aided in the strong initial attachment of both chitosan-BSA and TG-chitosan-BSA xerogels to the model mucoadhesive substrate.

The total work of adhesion (TWA) represented by the area under the curve also showed a statistically significant difference ($p < 0.0001$) between the v-BSA and TG-chitosan-BSA xerogels, with about threefold increase in mucoadhesive strength of the latter. Furthermore, the cohesiveness of the xerogels displayed a slight increase in the TG-chitosan based xerogels which was not significant. The major differences observed in the PAF, TWA and cohesiveness of the xerogels were attributed largely to the increased mucoadhesive strength impacted by the thiolation process via the formation of stronger ionic interactions between the cysteine-rich mucin glycoproteins and the sulfhydryl ligands of TG-chitosan. In addition, the formation of inter- and intra-molecular disulfide linkages within the TG-chitosan xerogels and the stability of the fibrous structure may have augmented the mucoadhesive strength. The relatively low mucoadhesive strength of the unmodified chitosan xerogels may have arisen from the excessive hydration of the porous structure leading to the formation of a slippery gel that lost its mucoadhesive strength. Mucoadhesive strength is a key property for the determination of the functional characteristic of residence time of xerogels at the absorption site to allow for sustained drug release and eventually bioavailability. Though significant differences were observed in the mucoadhesive performance of the xerogels, the differences were lower than those reported by Roldo, Hornof, Caliceti, and Bernkop-Schnürch (2004) where different formulation systems and bioadhesion membranes were used. It must however be emphasised that the process of thiolation greatly influenced the mucoadhesive performance.

3.8. In vitro drug dissolution studies

The dissolution profile of BSA from chitosan-BSA and TG-chitosan-BSA xerogels in 0.1 M PBS is shown in Fig. 6. The total cumulative percent BSA release from the chitosan-BSA and TG-chitosan-BSA were 91.5 ± 3.7% and 94.4 ± 7.3% respectively. This difference was not statistically significant ($p = 0.5$) with both formulations exhibiting classical sustained release profiles characteristic of chitosan based formulations. Drug release is facilitated by the porous network of lyophilised xerogels as a result of increased surface of dispersed drug within the porous cake which accelerates dissolution (Bunte et al., 2010). The similar release profiles from the xerogels exhibited a burst release of about 57% and 45% for chitosan and TG-chitosan respectively in the first 1 h, and then a constant controlled release. This could be attributed to two different release mechanisms; (a) diffusion of protein molecules and (b) degradation of polymer matrix. The initial BSA burst release was due to drug molecules adsorbed to the xerogel surface or loosely associated with the surface which easily diffused out in the initial incubation period of 1 h (Xu & Du, 2003). The movement of water molecules containing dissolved hydrophilic proteins is not restricted between the release medium and the polymer matrix (Kang & Song, 2008). The high loading concentration of BSA enhanced its release from the xerogels as the large concentration gradient between the release medium and the polymer surface resulted in a high diffusion rate. In addition, proteins dispersed within the polymer matrix may have escaped through cracks (pores) formed during processing, therefore increasing the initial release. A prolonged release period however, ensued after the initial burst release due to BSA-chitosan complexation. At pH 6.8, BSA (isoelectric point around 5) carries a net negative charge and complexes with positively charged chitosan. A slow diffusion of entrapped protein therefore occurred from hydrated chitosan and TG-chitosan xerogels (Wang, Shao, Meng, & Yang, 2010). Disulphide formation in TG-chitosan could have limited TG-chitosan-BSA complexation as less chitosan amino groups were available for interaction. Subsequently the TG-chitosan xerogel released more BSA than the chitosan xerogel though the difference was not statistically significant. The disulphide bond results in a stronger and stable swollen gel (maintained physical integrity) that displays excellent cohesive properties. The cohesion and stability of a drug delivery system over the intended duration of drug release is often a requirement for controlled release. The non-covalent complex however, gradually dissolves in the presence of NaCl (Boeris, Farruggia, & Picó, 2010) present in PBS which supports the higher % release of BSA observed in both xerogels.

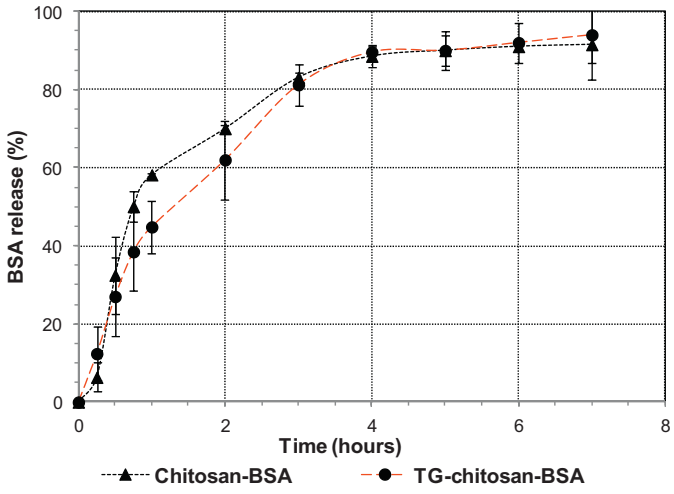

Fig. 6. Cumulative percent BSA release from annealed chitosan-BSA and TG-chitosan-BSA xerogels in 0.1 M PBS at 37 ± 0.1 °C ($n = 4$, mean ± S.D).

The usefulness of TG-chitosan as carrier matrices for controlled drug release has been demonstrated with model drugs such as metronidazole and clotrimazole (Saboktakin et al., 2011; Kast, Valenta, Leopold, & Bernkop-Schnürch, 2002).

4. Conclusions

Based on the structural integrity and characteristic performance after lyophilisation, a stable TG-chitosan based system for potential protein delivery via buccal mucosa has been developed. The characteristics of the drug loaded xerogels containing 6.5 mg each of plasticizer and cryoprotectant were influenced by the annealing and thiolation processes, which did not affect protein conformational stability. The various techniques used to characterise the lyophilised xerogels have indicated that the moisture content, swelling capacity, mucoadhesion properties and microscopic structure are influenced by the thiolation process. The annealing step in the lyophilisation cycle helped to obtain the desired porous structure for the xerogels. This had the advantage of increased ease of hydration, mucoadhesion and subsequently the drug release characteristics of the xerogels. The final lyophilised product was an elegant, mechanically strong cake and is expected to exhibit long-term storage stability. The principal implication of these findings is the potential application of the novel lyophilised thiolated chitosan for the delivery of proteins via the buccal mucosa and these will be investigated further in long-term stability evaluation and in an ex vivo and in vivo mucosal environment.

Conflict of interest

The authors report no conflict of interest.

Acknowledgements

The authors would like to thank the Commonwealth Scholarship Commission for funding the research studies. The commission played no part in the study design; the collection, analysis and interpretation of data; neither played any part in the writing of the report; and in the decision to submit this article for publication.

We are also grateful to Dr Ian Slipper for help in running of SEM and XRD experiments.

References

Andrew, G. P., Laverty, T. P., & Jones, D. S. (2009). Mucoadhesive polymeric platforms for controlled drug delivery. *European Journal of Pharmaceutics and Biopharmaceutics*, *71*(3), 505–518.

Ayensu, I., Mitchell, J. C., & Boateng, J. S. (2012). Development and physicomechanical characterisation of lyophilised chitosan wafers as potential protein drug delivery systems via the buccal mucosa. *Colloids and Surfaces B: Biointerfaces*, *91*, 258–265.

Bernkop-Schnürch, A. (2000). Chitosan, its derivatives: Potential excipients for peroral peptide delivery systems. *International Journal of Pharmaceutics*, *194*, 1–13.

Bernkop-Schnürch, A., Guggi, D., & Pinter, Y. (2004). Thiolated-chitosans: Development and *in vitro* evaluation of a mucoadhesive, permeation enhancing oral drug delivery system. *Journal of Controlled Release*, *94*, 177–186.

Boateng, J. S., Auffret, A. D., Matthews, K. H., Humphrey, M. J., Stevens, H. N. E., & Eccleston, G. M. (2010). Characterisation of lyophilised wafers and solvent evaporated films as potential drug delivery systems to mucosal surfaces. *International Journal of Pharmaceutics*, *389*(1–2), 24–31.

Boateng, J. S., Stevens, H. N. E., Eccleston, G. M., Auffret, A. D., Humphrey, M. J., & Matthews, K. H. (2009). Development and mechanical characterization of solvent-cast polymeric films as potential drug delivery systems to mucosal surfaces. *Drug Development and Industrial Pharmacy*, *35*, 986–996.

Boeris, V., Farruggia, B., & Picó, G. (2010). Chitosan-bovine serum albumin complex formation: A model to design an enzyme isolation method by polyelectrolyte precipitation. *Journal of Chromatography B*, *878*, 1543–1548.

Bunte, H., Drooge, D. J., Ottjes, G., Roukema, R., Verrijk, R., & Yessine, M. (2010). Key considerations when developing lyophilised formulation and current trends. *Pharmaceutical Technology Europe Digital*, *22*(3), 2–4.

Ernst, O., & Zor, T. (2010). Linearization of the Bradford protein assay. *Journal of Visualised Experiments*, 1–6. http://dx.doi.org/10.3791/1918

Grabovac, V., Guggi, D., & Bernkop-Schnürch, A. (2005). Comparison of the mucoadhesive properties of various polymers. *Advanced Drug Delivery Reviews*, *57*, 1713–1723.

Hornof, M. D., Kast, C. E., & Bernkop-Schnürch, A. (2003). In vitro evaluation of the viscoelastic behaviour of chitosan-thioglycolic acid conjugates. *European Journal of Pharmaceutics and Biopharmaceuticals*, *55*, 185–190.

Juntapram, K., Praphairaksit, N., Siraleartmukul, K., & Muangsin, N. (2012). Synthesis and characterization of chitosan-homocysteine thiolactone as a mucoadhesive polymer. *Carbohydrate Polymers*, *87*, 2399–2408.

Kang, G. D., & Song, S. (2008). Effect of chitosan on the release of protein from thermosensitive poly(organophosphazene) hydrogels. *International Journal of Pharmaceutics*, *349*, 188–195.

Kasper, J. C., & Freiss, W. (2011). The freezing step in lyophilisation: Physico-chemical fundamentals, freezing methods and consequences on process performance and quality attributes of biopharmaceutical. *European Journal of Pharmaceutics and Biopharmaceutics*, *78*, 248–263.

Kast, C. E., & Bernkop-Schnürch, A. (2001). Thiolated polymers–thiomers: Development and *in vitro* evaluation of chitosan-thioglycolic acid conjugates. *Biomaterials*, *22*, 2345–2352.

Kast, C. E., Valenta, C., Leopold, M., & Bernkop-Schnürch, A. (2002). Design and in vitro evaluation of a novel bioadhesive vaginal drug delivery system for clotrimazole. *Journal of Controlled Release*, *81*, 347–354.

Kelly, S. M., Jess, T. J., & Price, N. C. (2005). How to study proteins by circular dichroism. *Biochimica et Biophysica Acta-Proteins and Proteomics*, *1751*, 119–139.

Kumar, M. N. V. R., Muzzarelli, R. A. A., Muzzarelli, C., Sashiwa, H., & Domb, A. J. (2004). Chitosan chemistry and pharmaceutical perspectives. *Chemical Reviews*, *104*, 6017–6084.

Lee, D., Zhang, W., Shirley, S. A., Kong, X., Hellermann, G. R., Lockey, R. F., et al. (2007). Thiolated chitosan/DNA nanocomplexes exhibit enhanced and sustained gene delivery. *Pharmaceutical Research*, *24*(1), 157–167.

Leitner, V. M., Walker, G. F., & Bernkop-Schnürch, A. (2003). Thiolated polymers: Evidence for the formation of disulphide bonds with mucus glycoproteins. *European Journal of Pharmaceutics and Biopharmaceutics*, *56*, 207–214.

Muzzarelli, R. A. A., Boudrant, J., Meyer, D., Manno, N., DeMarchis, M., & Paoletti, M. G. (2012). Current views on fungal chitin/chitosan, human chitinases, food preservation, glucans, pectins and inulin: A tribute to Henri Braconnot, precursor of the carbohydrate polymers science, on the chitin bicentennial. *Carbohydrate Polymers*, *87*, 995–1012.

Nagahama, H., Maeda, H., Kashiki, T., Jayakumar, R., Furuike, T., & Tamura, H. (2009). Preparation and characterization of novel chitosan/gelatine membranes using chitosan hydrogel. *Carbohydrate Polymers*, *76*(2), 255–260.

Prabaharan, M., & Gong, S. (2008). Novel thiolated carboxymethyl chitosan-g-β-cyclodextrin as mucoadhesive hydrophobic drug delivery carriers. *Carbohydrate Polymers*, *73*, 117–125.

Qin, C., Li, H., Xiao, Q., Liu, Y., Zhu, J., & Du, Y. (2006). Water-solubility of chitosan and its antimicrobial activity. *Carbohydrate Polymers*, *63*, 367–374.

Quiming, N. S., Vergel, R. B., Nicolas, M. G., & Villanueva, J. A. (2005). Interaction of bovine serum albumin and metallothionein. *Journal of Health Science*, *51*, 8–15.

Roldo, M., Hornof, M., Caliceti, P., & Bernkop-Schnürch, A. (2004). Mucoadhesive thiolated chitosans as platforms for oral controlled drug delivery: Synthesis and *in vitro* evaluation. *European Journal of Pharmaceutics and Biopharmaceutics*, *57*(1), 115–121.

Saboktakin, M. R., Tabatabaie, R. M., Maharramov, A., & Ramazanov, M. A. (2011). Development and *in vitro* evaluation of thiolated-chitosan—Poly(methacrylic-acid) nanoparticles as a local mucoadhesive delivery system. *International Journal of Biological Macromolecules*, *48*, 403–407.

Snyder, G. H., Reddy, M. K., Cennerazzo, M. J., & Field, D. (1983). Use of local electrostatic environments of cysteines to enhance formation of a desired species in a reversible disulfide exchange reaction. *Biochimica et Biophysica Acta*, *749*, 219–226.

Solomonidou, D., Cremer, K., Krumme, M., & Kreuter, J. (2001). Effect of carbomer concentration and degree of neutralization on the mucoadhesive properties of polymer films. *Journal of Biomaterial Science: Polymer Edition*, *12*, 1191–1205.

Sreenivas, S. A., & Pai, K. V. (2009). Synthesis of thiolated chitosans: Promising polymers for prolonged mucoadhesive drug delivery. *International Journal of Pharmtech Research*, *1*(3), 670–678.

Thanou, M., Nihot, M. T., Jansen, M., Verhoef, J. C., & Junginger, J. C. (2001). Mono-N-carboxymethyl chitosan (MCC), a polyampholytic chitosan derivative, enhances the intestinal absorption of low molecular weight heparin across intestinal epithelia in vitro and in vivo. *Journal of Pharmaceutical Sciences*, *90*, 38–46.

Tiwari, D., Goldman, D., Sause, R., & Madan, P. L. (1999). Evaluation of polyoxyethylene homopolymers for buccal bioadhesive drug delivery device formulations. *AAPS PharmSci*, *1*, E13.

Wang, Y., Shao, J., Meng, Y., & Yang, Y. (2010). Controlled release of bovine serum albumin from chitosan membranes in vitro. *Medicinal Chemistry Research*, *19*, 1055–1063.

Xu, Y., & Du, Y. (2003). Effect of molecular structure of chitosan on protein delivery properties of chitosan nanoparticles. *International Journal of Pharmaceutics*, *250*, 215–226.